



1 **Increase in urban flood risk resulting from climate change – The role of storm temporal**
2 **patterns**

3 Suresh Hettiarachchi¹, Conrad Wasko¹, and Ashish Sharma^{1*}

4 ¹School of Civil and Environmental Engineering, University of New South Wales, Sydney,
5 Australia.

6 *Corresponding author, Prof. Ashish Sharma, A.Sharma@unsw.edu.au

7 **Abstract**

8 Warming temperatures are causing extreme rainfall to intensify resulting in increased risk of
9 flooding in developed areas. Quantifying this increased risk is of critical importance for the
10 protection of life and property as well as for infrastructure planning and design. The study
11 presented in this manuscript uses a comprehensive hydrologic and hydraulic model of a fully
12 developed urban/suburban catchment to explore two primary questions related to climate
13 change impacts on flood risk: (1) How does climate change effects on storm temporal
14 patterns and rainfall volumes impact flooding in a developed complex watershed? (2) Is the
15 storm temporal pattern as critical as the total volume of rainfall when evaluating urban flood
16 risk? The updated NOAA Atlas 14 intensity-duration-frequency (IDF) relationships and
17 temporal patterns, widely used in design and planning modelling in the USA, form the basis
18 of the assessment reported here. Current literature shows that a rise in temperature will result
19 in intensification of rainfall. These impacts are not explicitly included in the NOAA
20 temporal patterns, which can have consequences on the design and planning of adaptation
21 measures. We use the expected increase in temperature for the RCP8.5 scenario for 2081-
22 2100, to project temporal patterns and rainfall volumes to reflect future climatic change. The
23 modelling analysis for a 22 km² developed watershed show that temporal patterns cause
24 substantial variability in flood depths during a storm event. The changes in the projected
25 temporal patterns alone increase the risk of flood magnitude between 1 to 35 % with the
26 cumulative impacts of temperature rise on temporal pattern and the storm volume increasing
27 flood risk by between 10 to 170 % across the locations that were referenced for a 50 year
28 return period storm. The variability in catchment response to temporal patterns show that
29 regional storage facilities are sensitive to rainfall patterns that are loaded at the latter part of
30 the storm duration while the short duration extremely intense storms will cause extensive
31 flooding at all locations. This study shows that changes in temporal patterns will have a



32 significant impact on urban/suburban catchment response and need to be carefully considered
33 and adjusted to account for climate change when used for design and planning future
34 stormwater systems.

35 **Keywords:** Storm Temporal Patterns, Urban hydrology, Climate Change, urban flood risk.

36

37

38 **1 Introduction**

39 Recent history shows that extreme weather events are occurring more frequently and in areas
40 that have not had such events in the past (Hartmann et al., 2013). There are more land regions
41 where the number of heavy rainfall events has increased compared to where they have
42 decreased (Alexander et al., 2006; Donat et al., 2013; Westra et al., 2013a). A case study on
43 the Oshiwara River in Mumbai, India has shown a 22 % increase in the overall flood hazard
44 area within the catchment (Zope et al., 2016). Intensification of rainfall extremes (Lenderink
45 and van Meijgaard, 2008; Wasko and Sharma, 2015; Wasko et al., 2016b) and their
46 increasing volume (Mishra et al., 2012; Trenberth, 2011) has been linked to the higher
47 temperatures expected with climate change. This increase in the likelihood of extreme rainfall
48 and its intensification creates a higher risk of damaging flood events that cause a threat to
49 both life and the built environment, particular in urban regions where the existing
50 infrastructure has not been designed to cope with these increases. Adapting to future extreme
51 storm events (i.e. flood events) will likely be costly in both economic and social aspects
52 (Doocy et al., 2013). Properly addressing this increased flood risk is all the more important
53 given the expectation that the urban population is projected to grow from the current 54 %
54 to 66 % of the global population by the year 2050 (United Nations, 2014).

55 Adaptation as a way to address the effects of climate change has only recently gained
56 attention (Mamo, 2015). The effectiveness of adaptation is dependent on the accuracy of
57 simulating projected impacts, such as the effectiveness of a flood control structure to protect
58 a city from flooding in the future, and, the uncertainty in projected impacts, as this will limit
59 the amount of adaptation that society will accept (Adger et al., 2009). The foundation of
60 adaptation measures to deal with flooding is typically based on flood forecasting and
61 hydrologic/hydraulic (H/H) modelling (Thodsen, 2007). Prior to the advent of computers and
62 the increase in computational power, drainage design was based on simple models of peak



63 discharge rates using methods such as the rational formula in combination with
64 Intensity/Duration/Frequency (IDF) curves (Adams and Howard, 1986; Nguyen et al., 2010).
65 Consideration of the environmental impacts related to flow rates, volumes, water quality and
66 downstream impacts requires more complex systems and ways to simulate the hydrologic and
67 hydraulic processes in a more realistic manner (Nguyen et al., 2010). As such, the state of
68 the art in modelling urban sewer and stormwater related infrastructure uses distributed, fully
69 dynamic, hydrologic and hydraulics modelling software such as SWMM, infoWorks,
70 TUFLOW and MIKE packages (Singh and Woolhiser, 2002). The dynamic approach and
71 integrated nature of current modelling requires the use of temporal patterns to distribute
72 rainfall and volumes that closely resemble actual storm events (Nguyen et al., 2010; Rivard,
73 1996).

74 Temporal patterns have typically been derived using the alternating block method from IDF
75 curves where shorter storm durations are nested within longer storm duration design
76 intensities (García-Bartual and Andrés-Doménech, 2016; Victor Mockus and E. Woodward,
77 2015). However, this method does not represent a real storm structure. Alternatively, (Huff,
78 1967) presented the first rigorous analysis of rainfall temporal patterns (García-Bartual and
79 Andrés-Doménech, 2016), where rainfall temporal patterns were derived from observations.
80 Similar methods include the average variability method, where a storm is partitioned into
81 fractions of equal time, and each fraction is ranked. The temporal distribution is then
82 specified as the most likely rainfall order with the average rainfall used for the associated
83 fraction (Pilgrim, 1997). NOAA Atlas 14 provides an updated set of temporal distributions
84 and IDF curves for use in a major portion of the United States (Perica, 2013) that are now
85 widely used for planning and design modelling analysis. These temporal distributions and
86 rainfall depths are based on observed data and were generated using methodology similar to
87 (Huff, 1967). The major concern is that the analysis and methods used in Atlas 14 assumes a
88 stationary climate over the period of observation and application (Chapter 4.5.4 of Atlas 14
89 volume 8). This seems contrary to prevailing scientific thought (Milly et al., 2007) and can
90 lead to inadequacies of future stormwater infrastructure as there is evidence to believe that
91 warmer temperatures are forcing intensification of temporal patterns (Wasko and Sharma,
92 2015) and an increase in variability (Mamo, 2015). Several previous studies have examined
93 the sensitivity of urban catchments to changes in intensity and temporal patterns with peak
94 runoff rates and volumes modelled (Lambourne and Stephenson, 1987; Mamo, 2015; Nguyen
95 et al., 2010; Zhou et al., 2016). For example, Lambourne and Stephenson (1987) presented a



96 comparative model study to look at the impact of temporal patterns on peak discharge rates
97 and volumes. However, these studies largely ignored the detailed hydraulic conveyance
98 aspects of storage ponds, sewers, culverts, and flow control structures, with the exception of
99 (Zhou et al., 2016), which play an important role in how the flow rates generated during
100 runoff move through and impact on the built environment.

101 In this study, we focus on the range of results generated from detailed H/H modelling arising
102 from precipitation pattern variability and the impact of climatic change. In particular, we
103 focus on the temporal distribution of rainfall to assess and illustrate the variability in how
104 different catchments respond to different rainfall patterns. The primary questions that we
105 address are;

- 106 1. What is the relative importance of the storm pattern and volume of rainfall on urban
107 flood peaks?
- 108 2. How will climate change affect storm patterns and volumes and what are the impacts
109 on urban flood peaks?

110 **2. Impact of climate change on flooding in urban stormwater systems**

111 Developed urban areas present the highest probability of causing damage and loss of life
112 during flood events. There has been an increase in urban flooding in the past decade with
113 densely populated developing countries like India and China coming into focus (Bisht et al.,
114 2016; Zhou et al., 2017). In particular, flooding in Uttarakhand and Kashmir, which was
115 caused by extreme rainfall coupled with inadequate stormsewer design, is blamed for 580 and
116 200 deaths respectively (Bisht et al., 2016). China has also experienced a devastating flood
117 season in 2016 (Zhou et al., 2016) with the rapid increase in urbanization. Even with better
118 planned and mature urban cities, Europe and North America are not immune to flooding in
119 urban areas (Ashley et al., 2005; Feyen et al., 2009; Smith et al., 2016). The main
120 characteristic of stormwater in urban areas is that the flows are predominantly conveyed in
121 constructed systems, replacing or modifying the natural flow paths. Hence, the proper design
122 of these conveyance systems becomes crucial in managing flooding during extreme storms.
123 Impacts of climate change are expected to increase the risk of flooding and further exacerbate
124 the difficulty of flood management in developed environments.

125 The number of studies investigating climate change impacts on urban flooding is increasing
126 as the importance of this topic is more and more recognized. However, research focusing on



127 the impacts of climate change on precipitation temporal patterns remains limited. The
128 majority of available research use Global Circulation Models (GCMs) and Regional Climate
129 Models (RCMs) combined with statistical downscaling techniques to project IDF curves to
130 reflect future climate conditions (Mamo, 2015; Nguyen et al., 2010; Schreider et al., 2000).
131 For example Mamo (2015) used monthly mean wet weather scenario data projected by four
132 GCMs for the period 2020-2055, along with historic data from 1985 to 2013 to develop
133 revised IDF curves, which were then used as weather generator input using LAR-WG, from
134 which data was generated to develop the revised IDF curves. (Nguyen et al., 2010) used data
135 sets generated by two separate GCMs are used to develop IDF and temporal patterns to
136 reflect future rainfall patterns. The inconsistent results generated by the two different GCMs
137 in the (Nguyen et al., 2010) study illustrate the challenge of forecasting future climate
138 conditions with GCM generated results. It is recognized that GCM results form the largest
139 part of the uncertainty in projected flood scenarios (Prudhomme and Davies, 2009).

140 Alternatively, research has shown that temperature, which influences the amount of water
141 contained in the atmosphere, can have an impact on the patterns and total rainfall volumes of
142 storm events (Hardwick Jones et al., 2010b; Lenderink and van Meijgaard, 2008; Molnar et
143 al., 2015; Utsumi et al., 2011; Wasko et al., 2015; Westra et al., 2013a). In general,
144 intensification of rainfall events is expected with a trend towards ‘invigorating storm
145 dynamics’ (Trenberth, 2011; Wasko and Sharma, 2015). Even though forecasts for climate
146 change impacts on future flooding have a ‘low confidence’ global scale trends in temperature
147 extremes are more reliable (Seneviratne et al., 2012). Following successful studies (Wasko
148 and Sharma, 2017; Westra et al., 2013b) we take the approach of using temperature to project
149 temporal patterns and rainfall volume to account for climate change impacts. As described in
150 detail in section 3, we examine historical rainfall data coupled with daily average temperature
151 to project temporal patterns and rainfall volumes to account for climate change impacts.

152 Flood risk assessment and communication depend on flood risk mapping, for which flood
153 inundation areas are needed (Merz et al., 2010). Urban catchments are typically complex and
154 need to capture the response of the system along with the interactions of the various
155 components of the stormwater infrastructure (Zoppou, 2001) to provide reliable flood depths
156 to develop inundation areas. Including the complex hydraulics and possible hydraulic
157 attenuation and timing of congruent flows will have an impact on flooding, particularly in
158 developed environments. As mentioned, there are an increasing number of catchment/basin
159 scale and urban modelling studies that have been performed (Cameron, 2006; Graham et al.,



160 2007; Leander et al., 2008; Zhou et al., 2016; Zope et al., 2016). However, there is a lack of a
161 detailed study that looks at assessing future flood damage in a developed environment
162 (Seneviratne et al., 2012). The majority of these past studies focus on either the hydraulics
163 modelling component or the rainfall intensity aspect and mostly overlook the crucial detail of
164 rainfall patterns. As discussed, temporal patterns of rainfall is now a critical aspect of design
165 and planning of future storm systems. Research which uses temperature to project future
166 rainfall and associated temporal patterns of rainfall, and then assesses impacts on flooding
167 has not been performed. This study aims to fill this research gap through an elaborate
168 analysis of how rainfall intensities and patterns impact urban flood risk in a warmer climate.

169 **3. Study location, data and methodology**

170 This section describes the data and methods used to evaluate the variability in flood risk as
171 well as the impact to flood risk due to an increase in temperature. Broadly, the steps followed
172 are:

- 173 1 Apply multiple temporal patterns and rainfall volumes with their associated
174 confidence limits in the H/H model to establish the variability in the flood risk
- 175 2 Following (Lenderink and Attema, 2015; Wasko and Sharma, 2015) develop scaling
176 factors for the volume and temporal pattern for future conditions using temperature
177 as index
- 178 3 Evaluate impact of temperature rise on flood risk by scaling temporal patterns for a
179 temperature increase
- 180 4 Evaluate cumulative impact of temperature rise on flood risk by scaling volume and
181 temporal patterns

182 The hydrologic and hydraulic modelling presented in this paper was done using an EPA-
183 SWMM model of an urban/suburban catchment in Minneapolis, Minnesota, USA. The
184 SWMM software package was initially developed by the United States Environmental
185 Protection Agency (EPA, 2016) and has since been used as the base engine for most of the
186 industry standard H/H modelling packages.

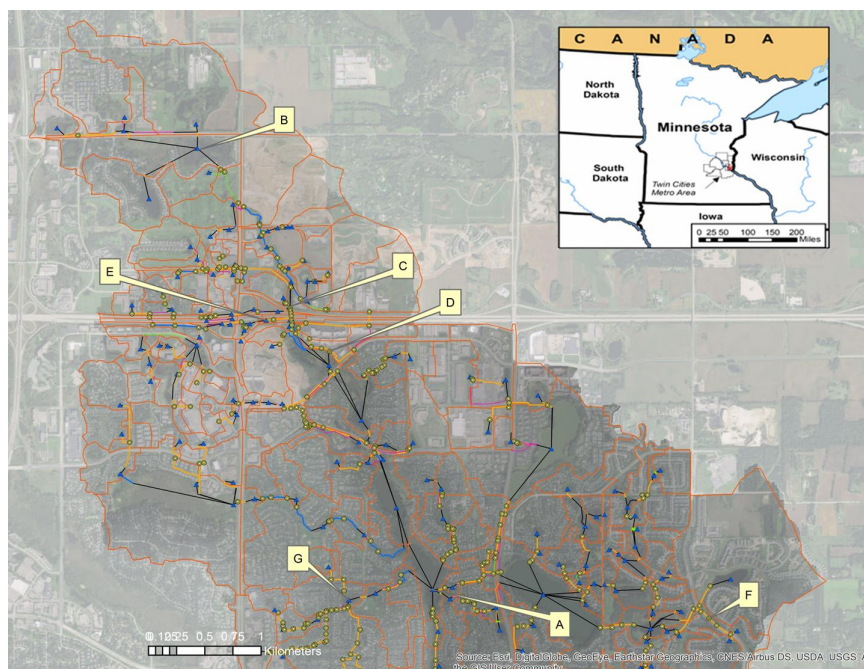
187 **3.1 Study Location and model**

188 The H/H model used in this study was developed for the South Washington Watershed
189 District (SWWD) in the State of Minnesota, USA for the management of surface water flows
190 and as well as land use planning and management. The catchment area of the SWWD is a



191 highly developed urban/suburban area and extends over 140-km². The model has extensive
192 detail of all landuse types and stormwater infrastructures including sewers, culvert crossing,
193 open channel reaches, and constructed as well as natural storages. For the purposes of this
194 study and to reduce the complexity and model run times, the model was trimmed to the upper
195 section of the SWWD representing an area of approximately 22 km². Figure 1 presents the
196 focus area. An important feature of this particular model is the level of detail of the
197 watershed storm sewer infrastructure as well as careful modelling of overflow routes to
198 capture all the flow during the peak. Figure 1 also shows the schematic of the model network
199 to illustrate the level of detail of the existing storm water infrastructure captured in the model.
200 This level of detail results in accurately modelling the travel time of flows within the
201 watershed and capturing all the runoff volume generated from the storm. The proper
202 simulation of hydraulic attenuation and a variety of landuse types provide an ideal platform
203 for this study.

204 Table 1 lists the primary reference locations that are used for this study. The locations have
205 specifically been chosen to represent the range of possible conditions that are encountered in
206 urban catchments. The sub-catchment sizes vary from less than 0.5 km² to approximately
207 2 km², with an overall catchment of 22 km². Different land uses such as commercial and
208 industrial or different types of residential areas, as well as the amount of storage, have all
209 been considered. It is important to note that these locations were selected prior to any model
210 runs or availability of results and hence do not bias the results presented. Table 1 gives a
211 description of the primary landuse type of the subwatershed that drains to each reference
212 location along with the watershed area and the overall percentage of impervious surface area
213 within that watershed. It also describes if there are local storage ponds, either natural or
214 constructed, that provide rate and volume control.



215

216 **Figure 1** Location of the model and the sub-watersheds along with the reference points used in the
 217 discussion below. The details of the reference points and further explanation are presented in Table 1

218 **Table 1.** Description of reference locations presented in Figure 1 and used to present results. Each
 219 location represents a variation of landuse within the watershed

| Reference point for results presented in figures | Landuse types and description | Watershed Area (km ²) | Average Percent impervious |
|--|--|-----------------------------------|----------------------------|
| (A) Wilmes | Natural lake and downstream limit of watershed. | ~ 22 | - |
| (B) Upstream | Predominantly rural, lower density residential landuse with good tree canopy and green spaces. Natural wetlands to mitigate flow with minimal to constructed storage | 2.2 | 32 |
| (C) Business park | Office space and parking lots with green space mixed in. Constructed storage and infiltration to help mitigate runoff | 0.5 | 42 |
| (D) Commercial 1 | Retail and parking dominates this area with some green spaces added in. Minimal constructed storage. Two | .25 | 60 |



| | | | |
|-------------------|--|------|----|
| | sub-surface infiltration basins installed under parking lots | | |
| (E) Commercial 2 | Retail and parking dominates this area with substantial constructed storage to help mitigate runoff rates and volumes. Part of the highway also drains through this point. | .75 | 48 |
| (F) Residential 1 | Medium density residential landuse with minimal constructed storage. | .35 | 24 |
| (G) Residential 2 | Medium density residential landuse with constructed storage. | 1.05 | 39 |

220

221 3.2 Precipitation and Temperature Data

222 The precipitation and temperature data used in the analysis were sourced from the National
223 Centers for Environmental Information hosted by the National Oceanic and Atmospheric
224 Administration (NOAA). Both hourly and daily rainfall data were downloaded from the
225 climate data online site for Minneapolis and St Paul (MSP) International Airport gauge,
226 which is the closest major airport to the study area. Daily data for the MSP airport was
227 available from 1901 through 2014, while hourly data was available from 1948 through 2014.
228 Daily maximum, minimum and average temperature data was also downloaded for the site
229 for the period from 1901 through 2014. For this analysis days that did not have precipitation
230 data were assumed to have no rain.

231 The temporal patterns for storms and the depths of rainfall were taken from NOAA ATLAS
232 14 volume 8 – the current state of the art design standard for this location. The modelling
233 analysis centred on the 50-year (2% exceedance probability) storm, which is a total rainfall
234 volume of 160 mm in 24-hours, for the area within the SWWD in the USA. The 90 %
235 confidence margin storm depths were added to the analysis to look at how flood depths
236 modelled vary with total precipitation (Table 2). Six temporal distributions (two patterns
237 with their associated confidence margins) were chosen from NOAA ATLAS 14 volume 8 to
238 investigate how flood depths are impacted by the shape of storm over a 24-hour period for
239 each of the above mentioned total rainfall depths. Table 2 describes the different storm
240 temporal patterns and each of the precipitation volumes modelled.



241 **Table 2. Description of notation used in reference to the modelled storm depths and**
 242 **temporal distributions (NOAA Atlas 14 volume 8 appendix 5)**

| Design Rainfall | Description |
|------------------|--|
| 160 mm 24 hour | 2 % exceedance 24-hour duration (50-year return period) rainfall depth |
| 12.5 cm 24 hour | Lower margin of the 90% confidence interval of the 2 % exceedance 24-hour duration (50-year return period) rainfall depth-Approximately Equivalent to the 20-year 24 hour ARI |
| 21 cm 24 hour | Upper margin of the 90% confidence interval of the 2 % exceedance 24-hour duration (50-year return period) rainfall depth-Approximately Equivalent to the 200-year 24 hour ARI |
| Temporal pattern | Description |
| Q1-10 - (a) | NOAA Midwest region, 1 st quartile 10 th percentile temporal distribution |
| Q1-50 - (b) | NOAA Midwest region, 1 st quartile 50 th percentile temporal distribution |
| Q1-90 - (c) | NOAA Midwest region, 1 st quartile 90 th percentile temporal distribution |
| Q3-10 - (d) | NOAA Midwest region, 3 rd quartile 10 th percentile temporal distribution |
| Q3-50 - (e) | NOAA Midwest region, 3 rd quartile 50 th percentile temporal distribution |
| Q3-90 - (f) | NOAA Midwest region, 3 rd quartile 90 th percentile temporal distribution |

243

244 The SWMM model was run for each of the precipitation amounts for the six temporal
 245 patterns, a total of 18 model runs, to generate the base dataset for current conditions and
 246 establish the variability in the current climate. The impact of climate change due to changed
 247 temporal patterns was assessed by modelling the 2% exceedance rainfall value (160 mm)
 248 with the temporal patterns that were scaled for an expected temperature increase (Section 3).
 249 Finally the cumulative impacts of changed temporal patterns and volume were evaluated by
 250 scaling both the rainfall volume and temporal patterns with temperature. An important point
 251 to note is that only the rainfall time series was changed appropriately for each model run. All
 252 the boundary conditions such as initial water levels at storage locations and all hydrologic
 253 parameters for each of the above model runs were kept the same for every model run.

254



255 **3.3 Temperature scaling of temporal patterns and rainfall volume**

256 To assess the impact of climate change, design storm temporal patterns and rainfall volumes
257 need to be projected for a future warmer climate. Most methods that project rainfall for future
258 climates focus on downscaling output from general circulation models to those required for
259 hydrological applications (Fowler et al., 2007; Maraun et al., 2010; Prudhomme et al., 2002)
260 through either dynamical or statistical models (Wilks, 2010). Downscaling methods however
261 will not replicate design rainfall (Woldemeskel et al., 2016), so an attractive alternative is that
262 proposed by (Lenderink and Attema, 2015) whereby historical temperature sensitivities
263 (scaling) are directly applied to the design rainfall.

264 Using established methods (Hardwick Jones et al., 2010a; Utsumi et al., 2011; Wasko and
265 Sharma, 2014), the volume scaling for the 24 hour storm duration was calculated using daily
266 rainfall paired with daily average temperature. The rainfall-temperature pairs were binned on
267 2 degree temperature bins and a Generalized Pareto Distribution fitted to the rainfall data in
268 each bin above the 99th percentile (Lenderink et al., 2011; Lenderink and van Meijgaard,
269 2008) to find extreme rainfall percentiles. A linear regression was subsequently fitted to the
270 fitted extreme percentiles and used as the rainfall volume scaling.

271 Temporal pattern scaling was calculated using hourly data, again paired to the average daily
272 temperature and followed the proposed methodologies in (Wasko and Sharma, 2015). The
273 largest 500 storm bursts of duration 24 hours were identified in the hourly data, with each
274 storm burst independent (not overlapping). The 24-hour duration storm bursts were divided
275 into 6 fractions, each fraction with duration of four hours. Each fraction was divided by the
276 rainfall volume and ranked from largest to smallest. An exponential regression was fitted to
277 the fractions corresponding to each rank and their corresponding temperature to produce a
278 temporal pattern scaling. The scaled temporal patterns were then applied and run through the
279 H/H models.

280 **4 Results and Discussion**

281 The results as discussed in the following section show that the variability in temporal
282 distributions of rainfall within a storm event can have significant impact on the level of
283 flooding. We show that the current industry standard temporal distributions need to be
284 adjusted to account for climate change impacts as do design rainfall volumes. The following
285 sections provide a detailed discussion of each step of the analysis.



286

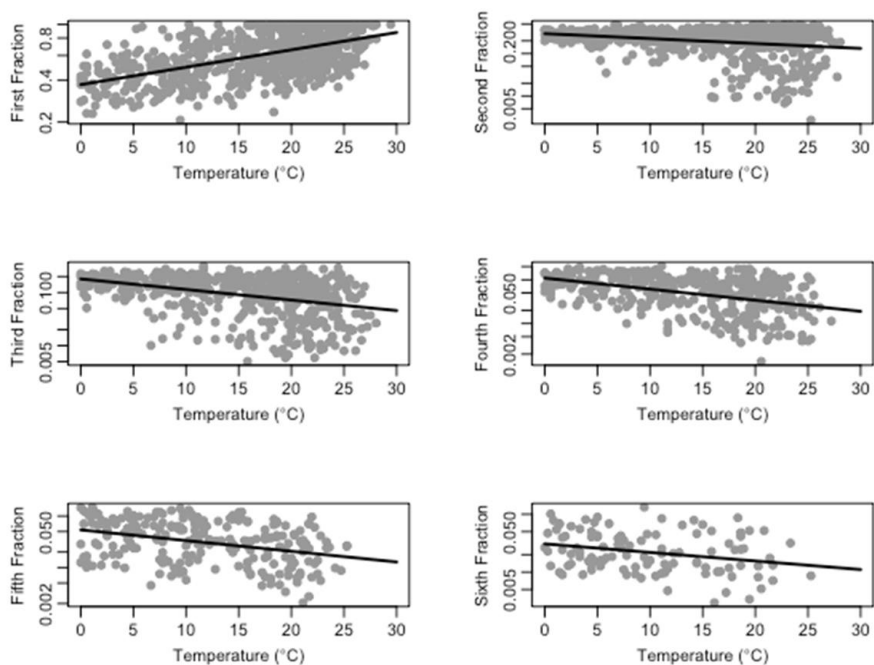
287 **4.1 Temporal patterns and volume scaling**

288 The scaling of the temporal pattern fraction for Minneapolis is presented in Figure 2. Table 3
289 provides the scaling that results from the fitted regression in each of the panels in Figure 2. A
290 temperature change of 5⁰C was selected to determine the percentage change based on
291 temperature increases estimated for the RCP8.5 scenario in Figure SPM7(a)(IPCC 2014)
292 projected for 2081-2100. As the slopes in Figure 2 and factors in Table 3 show, only the first
293 fraction scaled positively, which means that the 4 hours that included the highest amount of
294 rainfall scale up while the remaining rainfall fractions scale down. The results are consistent
295 with “invigorating storm dynamics” that are discussed in the literature (Lenderink and van
296 Meijgaard, 2008; Trenberth, 2011; Wasko and Sharma, 2015; Wasko et al., 2016b) resulting
297 in a less uniform, more intense storm. The percentage adjustments were normalized to make
298 sure that total rainfall amount did not change from the current value of 160 mm in 24-hours.
299 Figure 3 shows (Q1-50 and Q3-50 shown as an example) the changes to the temporal patterns
300 when the scaling percentages calculated above are applied. Figure 3 illustrates the change to
301 the highest peak rainfall rate and the decrease in the rest of the rainfall fractions. Similar
302 scaling was applied for all six temporal patterns that were used in the H/H modelling
303 analysis. As an additional verification, a similar analysis was completed for two
304 neighbouring locations (Sioux Falls South, Dakota and Milwaukee, Wisconsin). The fraction
305 and volume scaling results for both Sioux Falls and Milwaukee were consistent with those
306 discussed in this paper.

307 Figure 4 presents the precipitation volume temperature pairs, the extreme percentiles
308 generated based on the temperature bins, as well as the resulting scaling for the 24 hour
309 rainfalls. The daily total rainfall of 160 mm fell into the 99.99th percentile based on a cursory
310 ranking of the daily precipitation data. Hence, the 99.99th percentile 2.92 % scaling was
311 selecting for the 24 hour volume. This is broadly consistent with (Utsumi et al., 2011) and
312 (Wasko et al., 2016a) who present scaling between 2 and 5 % for the central north of the U.S
313 for the 99th percentile and throughout Australia. This value is less than the scaling found by
314 (Mishra et al., 2012) who used hourly precipitation, which is consistent with the expectation
315 that shorter duration extremes scale more (Hardwick Jones et al., 2010a; Panthou et al., 2014;
316 Wasko et al., 2015). This scaling converts to an approximately 20 % increase in the volume
317 of rainfall for a 24 hour period for a five degree increase. Applying the 20 % increase to the



318 160 mm in 24-hours gives a rainfall depth of 208 mm in 24 hours. Coincidentally, 208
 319 mm (~210 mm) in 24 hours is the upper margin of the 90% confidence interval for the 160
 320 mm event based on the margin provided in NOAA Atlas 14.



321

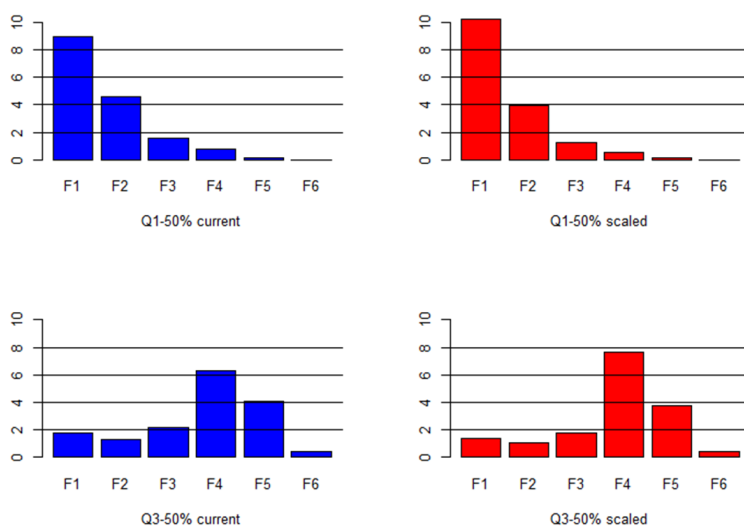
322 **Figure 2. Scaling temporal pattern fractions with temperature for Minneapolis (1948-2014 hourly data).**

323 **Black lines represent the fitted exponential regression.**

324 **Table 3 Temporal pattern scaling factors for each of the fractions**

| Fraction | Scaling factor |
|----------|----------------|
| F1 | 0.029 |
| F2 | -0.026 |
| F3 | -0.045 |
| F4 | -0.057 |
| F5 | -0.047 |
| F6 | -0.033 |

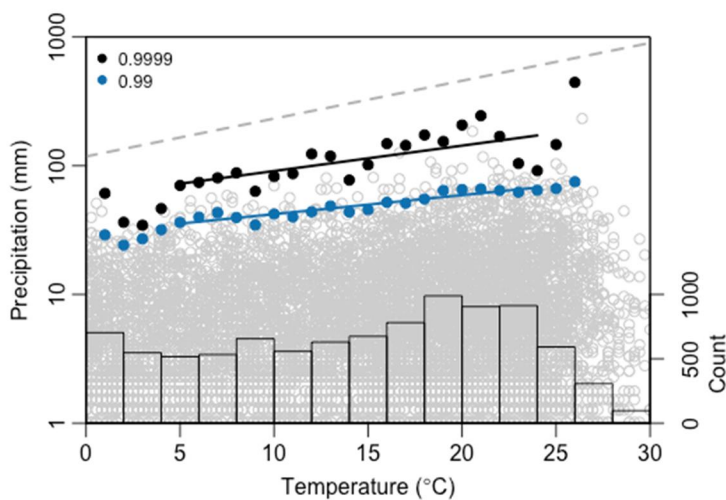
325



326

327 **Figure 3** Q1-50 and Q3-50 temporal patterns projected for temperature rise of 5⁰ C. Total rainfall of 160
 328 mm over 24 hours with each fraction representing accumulated rain for 4-hour periods.

329



330

331 **Figure 4** Scaling total volume of rainfall with temperature for Minneapolis (1901-2014 daily rainfall
 332 data). The grey dashed line represents a scaling of 7 %. The histogram represents the number of
 333 precipitation-temperature pairs.



334

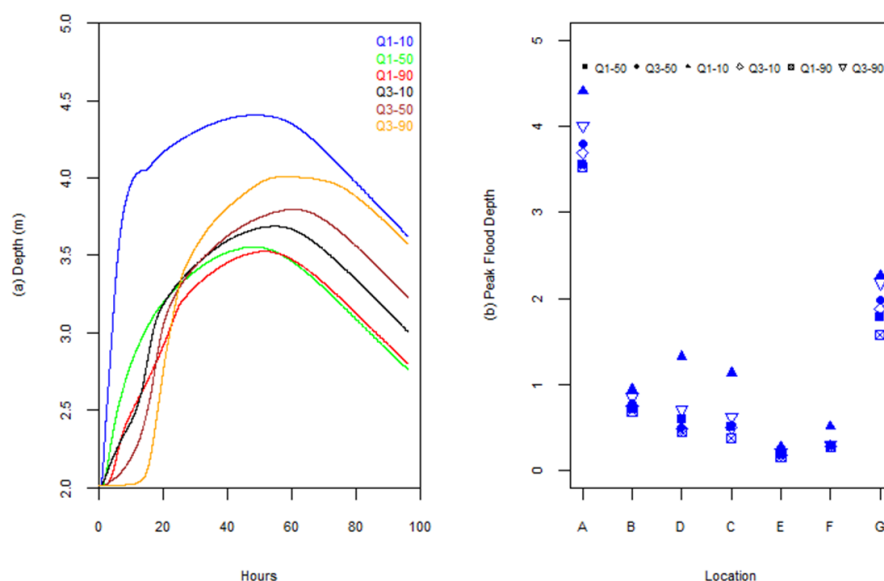
335 **4.2 Flood depth response to temporal patterns and total rainfall variability.**

336 The hydrologic/hydraulic model was run for the 18 different combinations of rainfall
337 volumes and temporal patterns. Results are presented for the five reference locations
338 throughout the watershed that represent different landuse types that are typical in a developed
339 area as described in Table 2. The flood depths extracted from the model were first analysed
340 to compare variability between temporal patterns and total rainfall depth. The selection of
341 the reference points essentially provides results at different sub-catchments, or different sub-
342 models. These sub-models show the variation in catchment response to runoff generated by
343 different land use types as well as how the flows then move through the different stormwater
344 infrastructure.

345 Figures 5(a) shows the depth/time curve at Wilmes Lake (location A) which is the main
346 regional collection point and the downstream end of the model. Each curve represents
347 change in depth versus time for the six temporal patterns distributing the same total rainfall
348 volume of 160 mm. The differences in shape, peak flood depth and the time to peak illustrate
349 the variability of flooding that can result purely due to variation in in-storm rainfall pattern.
350 A striking result is the approximately 30 % (1.3 m) variation in flood depth (relative to mean
351 flood depth) at Wilmes Lake purely due to variation of how the rain falls within the duration
352 of the storm. Not surprisingly, the highest flood depth curve is a result of the most intense
353 storm event pattern which is the Q1-10 distribution. The depth at Wilmes Lake rises quickly
354 during the Q1-10 event and then stays high for the longest duration. The high intensity of the
355 Q1-10 pattern can overwhelm local conveyance and storage structures, resulting in
356 uncontrolled overflow along city streets that flushes flow down to the low lying areas very
357 quickly, causing the water level at the lake to rise. Interestingly the next highest peak flood
358 level results from the Q3 pattern which has the majority of the precipitation loaded at the
359 latter half of the storm event. This type of pattern results in higher runoff volume as the soil
360 saturates and infiltration rates are reduced as well as local storage structures and ponds fill up
361 by the time the bulk of the storm occurs. This suggests that, on average, regional storage
362 facilities such as Wilmes Lake within the SWWD are more sensitive to the runoff volume
363 than the instantaneous peak flow rate, and thereby more sensitive to end loaded temporal
364 patterns during storms.

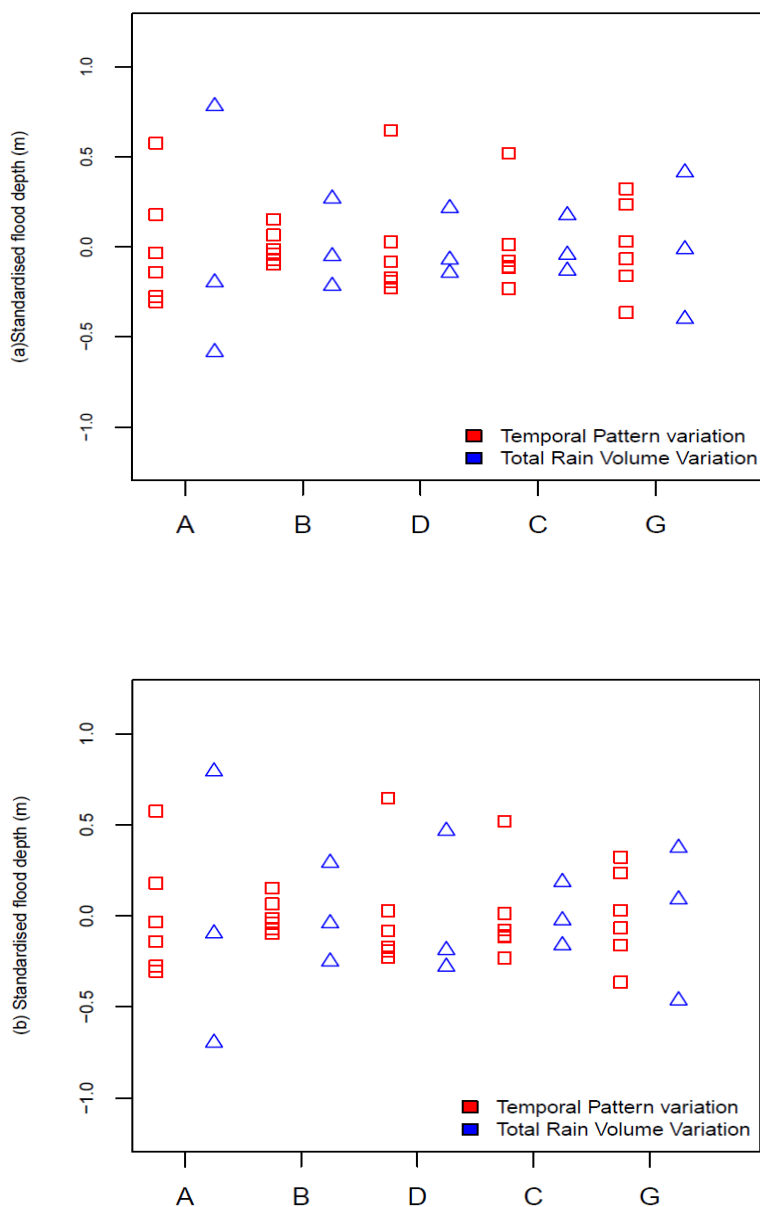


365 Figure 5(b) illustrates the same type of variation of peak flood depth due to the different
366 temporal patterns at each of the reference points. There is appreciable variation in peak flood
367 depths at all locations with the smallest range at location B. As described in Table 1, location
368 B has more rural landuse with local natural storage, which can explain the lack of variability
369 in flood depth relative to changes in temporal patterns. The range of variation in flood peaks
370 at locations C and D suggest that catchments with higher impervious have a higher sensitivity
371 to rainfall patterns. Locations F and G are both residential catchments though the area
372 draining to location G is larger. Additionally, locations F is a manhole within the storm
373 sewer system while location G is local constructed pond, which suggests that variation in
374 flow rates, or peak runoff from a catchment, does not always translate to higher variation in
375 flood depths. In general, Figure 5(b) illustrates that temporal patterns of rainfall can lead to
376 substantial variability in flood depths.



377

378 **Figure 5 (a) Depth over time at Wilmes Lake (Location A), which is the downstream regional**
379 **reference point in Figure 1. Depth vs time curves are plotted for 160 mm of total rainfall over 24**
380 **hours with the six temporal patterns. (b) Presents the variation of peak flood depth at reference**
381 **locations throughout the watershed (ref to table 1) with variation of temporal patterns for a total**
382 **of 160 mm of rainfall over 24 hours.**



383

384

385 **Figure 6 Comparison of total volume of rainfall and temporal patterns variability impact on peak flood**
386 **depth (a) Flood depth variation due to the 6 different temporal patterns with 160 mm of rain compared to**
387 **110, 160 and 210 mm of total rainfall over 24 hours distributed over a Q1-50 temporal pattern. (b) Flood**
388 **depth variation due to the 6 different temporal patterns with 160mm of rain compared to 110, 160 and**



389 **210 mm of total rainfall over 24 hours distributed over a Q3-50 temporal pattern. Flood depths were**
390 **standardised by subtracting the mean at each location for ease of comparison**

391 One of the primary questions that we set out to answer was the comparison of “how it rains”
392 versus “how much it rains”. For clarification, “how it rains” refers to the variation of
393 temporal patterns during a storm event with the total rainfall volume for the storm event held
394 constant. The term “how much it rains” refers to different volumes of rainfall for each storm
395 event with the temporal pattern held constant. Figure 6 (a) and (b) make the direct
396 comparison between the variations of peak flood depth between “how it rains” versus “how
397 much it rains”. The range in peak depths at the reference locations indicates how the
398 different catchments respond to variability in storm volume and pattern.

399 Location A is the regional concentration point and as shown in Figure 5(a), flood depths here
400 are more sensitive to total rainfall volume. It is interesting that the different temporal patterns
401 did generate a comparable range in variation of flood depths at location A. Locations C and
402 D have higher impervious surface area within the sub-watershed and show a wider range in
403 flood depths due to temporal patterns. Location G, which represents a residential area
404 responds more to variation in total rainfall volume. One of the interesting observations from
405 Figure 6 is that the change in rainfall volume results in a larger variability when applied to a
406 Q3 temporal pattern (Figure 6(b)). The general variability due to temporal patterns is higher
407 when compared to a total rainfall volumes distributed over a Q1 temporal pattern.
408 Combining these observations suggests that the changes in total rainfall volume have a bigger
409 impact when the peak of the storm arrives at the latter half of the event. The results in Figure
410 6 clearly indicate that temporal patterns of storms play a significant role in watershed
411 response to storm events. It is also clear that temporal patterns have to be carefully
412 considered when looking at flood depths and extents, especially in complex and developed
413 watersheds. In addition the range in the results shown in Figure 4 and 5 illustrate the
414 importance of considering “how it rains” when trying to quantify uncertainties related to H/H
415 modelling. This is especially a concern given the evidence to date that systematic change is
416 occurring to rainfall patterns across climate zones, making them more intense and impactful
417 in derived flood estimations (Wasko and Sharma, 2015).

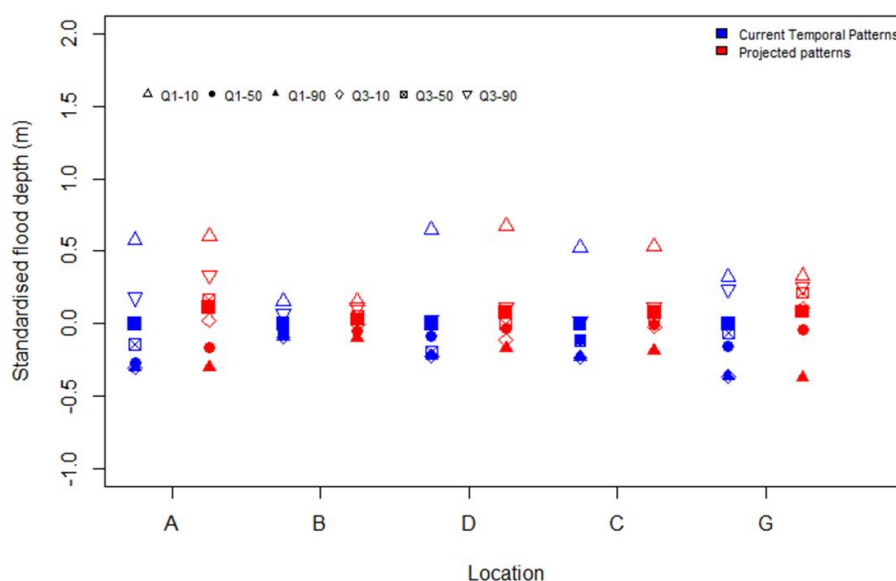
418

419



420 **4.3 Impact of applying temperature scaling to temporal patterns and rainfall volume**
 421 **on flood depths**

422 Figure 7 compares the results for projected temporal patterns with results from the base
 423 simulation. Both scenarios are based on the 50 year return period event which is 160 mm
 424 distributed over the six base and projected temporal patterns. The depth results shown in
 425 Figures 7 are variation of the peak flood depth around the mean of the results from the base
 426 conditions models. In other words, the depth results were standardized by subtracting the
 427 mean of the base conditions results from the results at each location.



428

429 **Figure 7. Impact of rise in temperature on the peak flood depth variation at reference locations within the**
 430 **watershed when scaling applied only to temporal patterns. The peak flood depths at each reference point**
 431 **are based on 160 mm of total rain distributed over the 6 temporal patterns used. Temperature scaling**
 432 **(T/S) for the temporal patterns are based scaling fractions presented in Figure 4. Flood depths were**
 433 **standardised by subtracting the mean from the base simulations presented in Figure 6 for each location.**

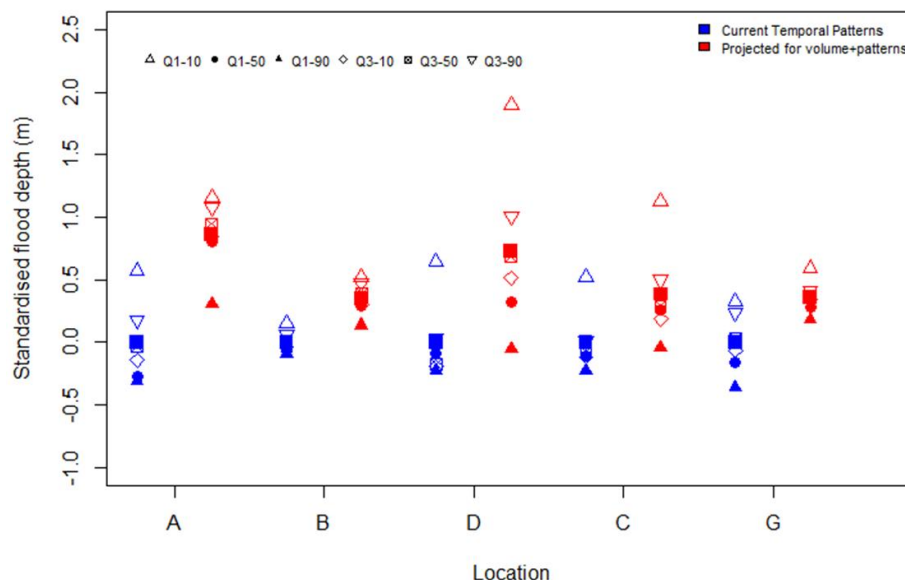
434 There is an increase in peak flood depth with the projection of temporal patterns alone
 435 (Figure 7). Unsurprisingly, the highest flood depth results from the Q1-10 pattern for both
 436 current and scaled conditions. But the results at the highest depths show little change due to
 437 temperature scaling of the Q1-10 pattern. The Q1-10 pattern is an extremely high intensity



438 event with majority of the rainfall occurring in the first fraction of the event. Applying the
439 scaling to this fraction makes minimal changes to the overall pattern of rainfall. Interestingly,
440 there is minimal to no change in the range of flood depths at each location due to the different
441 projected temporal patterns when compared to the current conditions results. The change in
442 mean flood depth is within the current overall variability of the results. Alternatively, if we
443 take the extreme Q1-10 event out of consideration, one can say that qualitatively the mean of
444 the flood depth for projected events does exceed the upper limit of the variability in flood
445 depths for the base scenario.

446 The important fact is that these plots are based on the same total rainfall volume of 160 mm.
447 All the variability is purely due to the differences in temporal patterns. The increase in mean
448 flood depth in the projected condition is purely due to changes to the base temporal patterns
449 and not due to any increase in rainfall volume. The mean of the peak flood depths does shift
450 up at each location even with the differences in catchment characterises. This clearly provides
451 the answers to the questions that were initially set, that the temporal patterns are an important
452 factor that needs careful consideration and that climate change impacts on these temporal
453 patterns will increase the likelihood of flooding in the future.

454 Figure 8 shows the same comparison as in Figure 7 when temperature scaling is applied to
455 both the temporal pattern and rainfall volume. Hence Figure 8 presents the cumulative
456 impacts of temperature scaling to the base conditions. As in Figure 7, the results in Figure 8
457 show the variation of results for both scenarios around the mean of the base condition flood
458 depth at each location.



459

460 **Figure 8. Impact of rise in temperature on the peak flood depth variation at reference locations within the**
461 **watershed, when scaling applied to both rainfall volume and temporal pattern. The peak flood depths at**
462 **each reference point are based on 210 mm of total rain distributed over the 6 temporal patterns used.**
463 **Flood depths were standardised by subtracting the mean from the base simulations presented in Figure 6**
464 **for each location.**

465 As expected, substantial increase in flood risk is seen when the cumulative impacts of
466 changes to temporal pattern and increase in precipitation volume due to temperature rise are
467 modelled. The mean flood depth is outside the upper margin of the highest flood depth for
468 base conditions except at the business park (C). The business park location (C) comes close
469 to meeting this threshold as well. The mean flood depth at Wilmes Lake (A) increases by
470 approximately 1 m, which translates to a significant increase in the extent of flooding. The
471 biggest change due to cumulative impacts occurs at the upstream location (B) were
472 previously, when only the temporal patterns were scaled, minimal impact was shown.
473 Additionally, the range of the results and the overall variability has increased at the
474 commercial and business park areas (C, D) locations when compared to Figure 7. The higher
475 intensity and the larger total volume of rainfall overwhelm the existing infrastructure with
476 much larger surface overflows that increase the flood risk.



477 The increase in flood depth at the reference locations due to changes to temporal patterns
478 alone range from 1 % to 35 %, while the cumulative impacts increase flood depth from 10 %
479 to as much as 170 %. When considering all the nodes in the model, the average increase in
480 flood depth due to changes in temporal patterns was 6 %. Similarly the average increase in
481 flood depth throughout the entire model due to cumulative impacts of both changes to
482 temporal pattern and rainfall volume is 37 %. The percentage increase shows that there is a
483 significant impact to overall flood risk throughout the catchment and that it is not isolated to
484 the reference points that are discussed in detail.

485 As mentioned above, the process of characterizing the way a catchment responds during a
486 storm event and how the flows interact with the built environment in an urban setting is
487 highly complex and variable. The variation of reference locations selected for this study
488 provides a reasonable assessment of how the flows interact with the physical features of the
489 catchment and how the results differ based on the location and features. This study clearly
490 shows the sensitivity of the catchment to variation in how it rains, in particular the areas that
491 are more impacted by volume as opposed to flow rate. Explicitly including intensification of
492 rainfall patterns and volume due to climate change along with detailed H/H modelling to
493 assess the variability in catchment response makes this study unique among available
494 literature. The methodology presented here is universally applicable and the benefits of
495 correctly designing infrastructure are likely to far outweigh the cost of the added effort, even
496 in industry applications

497

498 **5 Conclusions**

499 The significance of temporal patterns and how climate change impacts on rainfall patterns
500 affect flooding in developed environments was investigated using detailed hydrologic and
501 hydraulic modelling. Climate change impacts were undertaken by projecting historical
502 precipitation-temperature sensitivities on storm volumes and temporal patterns. The
503 following conclusions can be drawn from the results presented;

- 504 1. The response of a complex catchment is sensitive to variability in rainfall temporal
505 pattern. The flood depths varied in excess of 1 m at Wilmes Lake when different
506 temporal patterns were used with a constant volume of precipitation.



- 507 2. The variability due to temporal pattern had similar magnitude when compared to
508 variability due to total rainfall volume, which clearly shows that the temporal pattern
509 of rainfall is as important as the volume of rainfall for the purposes of H/H modelling.
510 3. The temporal patterns intensified when scaled based on estimated temperature
511 increases due to climate change.
- 512 4. A 1 % to 35 % increase in flood depth resulted when the scaled temporal patterns
513 were used in the H/H model, suggesting an increase in potential flood risk purely due
514 changes to “how it rains” as a result of climate change impacts.
- 515 5. A 10 % to 170 % increase in flood depth resulted when the projected rainfall volume
516 was added to the projected temporal patterns.
- 517 6. The variability of flood depth at each location also increased suggesting that H/H
518 modelling for future planning and design needs to give serious consideration to the
519 aspects of variability of rainfall patterns as well as increase in rainfall amounts.
- 520 7. The study shows that regional storage facilities are sensitive to rainfall patterns that
521 are loaded at the latter part of the storm duration while the extremely intense storms
522 will cause flooding at all locations.

523 The effect of projected intensification of storms due to climate change impacts suggests that
524 action needs to be taken promptly to prevent flood damages and possible loss of life. The two
525 most important points that can be derived from this study is that temporal patterns and storm
526 volumes need to be adjusted to account for climate change when applying to models of future
527 scenarios. The general application of H/H modelling analysis needs to adopt an ensemble
528 approach rather than a single event model to consider the significant variability in rainfall
529 patterns that can generate a substantial range in results in order to make a properly informed
530 decision as shown in this paper.

531 **Acknowledgments**

532 The authors acknowledge and thank the South Washington Watershed District
533 (<http://www.swwdmn.org>) in Minnesota, USA for providing the model as well as the
534 background data used for the analysis. We also acknowledge financial support of the
535 Australian Research Council. The rainfall and temperature data for Minneapolis Airport and
536 locations around the site were taken from <https://www.ncdc.noaa.gov/cdo-web/>. NOAA Atlas
537 14 Volume 8 is available at http://www.nws.noaa.gov/oh/hdsc/PF_documents



538 Technical details of EPA-SWMM can be found at [https://www.epa.gov/water-](https://www.epa.gov/water-research/storm-water-management-model-swmm)
539 [research/storm-water-management-model-swmm](https://www.epa.gov/water-research/storm-water-management-model-swmm).

540

541 **References**

542 Adams, B. J. and Howard, C. D.: Design storm pathology, Canadian Water Resources
543 Journal, 11, 49-55, 1986.

544

545 Adger, W. N., Dessai, S., Goulden, M., Hulme, M., Lorenzoni, I., Nelson, D. R., Naess, L.
546 O., Wolf, J., and Wreford, A.: Are there social limits to adaptation to climate change?,
547 Climatic Change, 93, 335-354, 2009.

548

549 Alexander, L. V., Zhang, X., Peterson, T. C., Caesar, J., Gleason, B., Tank, A. M. G. K.,
550 Haylock, M., Collins, D., Trewin, B., Rahimzadeh, F., Tagipour, A., Kumar, K. R.,
551 Revadekar, J., Griffiths, G., Vincent, L., Stephenson, D. B., Burn, J., Aguilar, E., Brunet, M.,
552 Taylor, M., New, M., Zhai, P., Rusticucci, M., and Vazquez- Aguirre, J. L.: Global observed
553 changes in daily climate extremes of temperature and precipitation, Journal of Geophysical
554 Research: Atmospheres (1984–2012), 111, 2006.

555

556 Ashley, R. M., Balmforth, D. J., Saul, A. J., and Blanskby, J.: Flooding in the future–
557 predicting climate change, risks and responses in urban areas, Water Science and
558 Technology, 52, 265-273, 2005.

559

560 Bisht, D. S., Chatterjee, C., Kalakoti, S., Upadhyay, P., Sahoo, M., and Panda, A.: Modeling
561 urban floods and drainage using SWMM and MIKE URBAN: a case study, Natural Hazards,
562 84, 749-776, 2016.

563

564 Cameron, D.: An application of the UKCIP02 climate change scenarios to flood estimation
565 by continuous simulation for a gauged catchment in the northeast of Scotland, UK (with
566 uncertainty), Journal of Hydrology, 328, 212-226, 2006.

567

568 Donat, M. G., Alexander, L. V., Yang, H., Durre, I., Vose, R., Dunn, R. J. H., Willett, K. M.,
569 Aguilar, E., Brunet, M., Caesar, J., Hewitson, B., Jack, C., Tank, A. M. G. K., Kruger, A. C.,
570 Marengo, J., Peterson, T. C., Renom, M., Rojas, C. O., Rusticucci, M., Salinger, J., Elayah,
571 A. S., Sekele, S. S., Srivastava, A. K., Trewin, B., Villarroel, C., Vincent, L. A., Zhai, P.,
572 Zhang, X., and Kitching, S.: Updated analyses of temperature and precipitation extreme
573 indices since the beginning of the twentieth century: The HadEX2 dataset, Journal of
574 Geophysical Research: Atmospheres, 118, 2098-2118, 2013.

575

576 Doocy, S., Daniels, A., Murray, S., and Kirsch, T.: The Human impact of floods: a historical
577 review of events 1980-2009 and systematic literature review, PLoS Curr, Disasters, 5, 2013.
578 EPA, U.: Storm Water Management Model, 2016. 2016.

579

580 Feyen, L., Barredo, J., and Dankers, R.: Implications of global warming and urban land use
581 change on flooding in Europe, Water & Urban Development Paradigms-Towards an
582 integration of engineering, design and management approaches, 2009. 217-225, 2009.



- 583 Fowler, H. J., Blenkinsop, S., and Tebaldi, C.: Linking climate change modelling to impacts
584 studies: recent advances in downscaling techniques for hydrological modelling, *International*
585 *Journal of Climatology*, 27, 1547-1578, 2007.
586
- 587 García-Bartual, R. and Andrés-Doménech, I.: A two parameter design storm for
588 Mediterranean convective rainfall, *Hydrology and Earth System Sciences Discussions*, doi:
589 10.5194/hess-2016-644, 2016. 1-19, 2016.
590
- 591 Graham, L. P., Andréasson, J., and Carlsson, B.: Assessing climate change impacts on
592 hydrology from an ensemble of regional climate models, model scales and linking methods –
593 a case study on the Lule River basin, *Climatic Change*, 81, 293-307, 2007.
594
- 595 Hardwick Jones, R., Westra, S., and Sharma, A.: Observed relationships between extreme
596 sub-daily precipitation, surface temperature, and relative humidity, *Geophysical Research*
597 *Letters*, 37, n/a-n/a, 2010a.
598 Hardwick Jones, R., Westra, S., and Sharma, A.: Observed relationships between extreme
599 sub- daily precipitation, surface temperature, and relative humidity, *Geophysical Research*
600 *Letters*, 37, 2010b.
601
- 602 Hartmann, D. L., Klein Tank, A. M., Rusticucci, M., Alexander, L. V., Brönnimann, S.,
603 Charabi, Y. A. R., Dentener, F. J., Dlugokencky, E. J., Easterling, D. R., and Kaplan, A.:
604 *Climate Change 2013 the Physical Science Basis: Working Group I Contribution to the Fifth*
605 *Assessment Report of the Intergovernmental Panel on Climate Change*, 2013.
606
- 607 Huff, F. A.: Time distribution of rainfall in heavy storms, *Water Resources Research*, 3,
608 1007-1019, 1967.
609
- 610 Lambourne, J. J. and Stephenson, D.: Model study of the effect of temporal storm
611 distributions on peak discharges and volumes, *Hydrological Sciences Journal*, 32, 215-226,
612 1987.
613
- 614 Leander, R., Buishand, T. A., van den Hurk, B. J., and de Wit, M. J.: Estimated changes in
615 flood quantiles of the river Meuse from resampling of regional climate model output, *Journal*
616 *of Hydrology*, 351, 331-343, 2008.
617
- 618 Lenderink, G. and Attema, J.: A simple scaling approach to produce climate scenarios of
619 local precipitation extremes for the Netherlands, *Environmental Research Letters*, 10,
620 085001, 2015.
621
- 622 Lenderink, G., Mok, H., Lee, T., and Van Oldenborgh, G.: Scaling and trends of hourly
623 precipitation extremes in two different climate zones–Hong Kong and the Netherlands,
624 *Hydrology and Earth System Sciences*, 15, 3033-3041, 2011.
625
- 626 Lenderink, G. and van Meijgaard, E.: Increase in hourly precipitation extremes beyond
627 expectations from temperature changes, *Nature Geoscience*, 1, 511-514, 2008.
628 Mamo, T. G.: Evaluation of the Potential Impact of Rainfall Intensity Variation due to
629 Climate Change on Existing Drainage Infrastructure, *Journal of Irrigation and Drainage*
630 *Engineering*, 141, 05015002, 2015.
631



- 632 Maraun, D., Wetterhall, F., Ireson, A. M., Chandler, R. E., Kendon, E. J., Widmann, M.,
633 Brienen, S., Rust, H. W., Sauter, T., Themeßl, M., Venema, V. K. C., Chun, K. P., Goodess,
634 C. M., Jones, R. G., Onof, C., Vrac, M., and Thiele- Eich, I.: Precipitation downscaling
635 under climate change: Recent developments to bridge the gap between dynamical models and
636 the end user, *Reviews of Geophysics*, 48, 2010.
- 637
- 638 Merz, B., Kreibich, H., Schwarze, R., and Thielen, A.: Review article " Assessment of
639 economic flood damage", *Natural Hazards and Earth System Sciences*, 10, 1697, 2010.
- 640
- 641 Milly, P., Julio, B., Malin, F., Robert, M., Zbigniew, W., Dennis, P., and Ronald, J.:
642 Stationarity is dead, *Ground Water News & Views*, 4, 6-8, 2007.
- 643
- 644 Mishra, V., Wallace, J. M., and Lettenmaier, D. P.: Relationship between hourly extreme
645 precipitation and local air temperature in the United States, *Geophysical Research Letters*, 39,
646 2012.
- 647
- 648 Molnar, P., Fatichi, S., Gaál, L., Szolgay, J., and Burlando, P.: Storm type effects on super
649 Clausius–Clapeyron scaling of intense rainstorm properties with air temperature, *Hydrol.*
650 *Earth Syst. Sci.*, 19, 1753-1766, 2015.
- 651
- 652 Nguyen, V. T., Desramaut, N., and Nguyen, T. D.: Optimal rainfall temporal patterns for
653 urban drainage design in the context of climate change, *Water Sci Technol*, 62, 1170-1176,
654 2010.
- 655
- 656 Panthou, G., Mailhot, A., Laurence, E., and Talbot, G.: Relationship between surface
657 temperature and extreme rainfalls: A multi-time-scale and event-based analysis, *Journal of*
658 *Hydrometeorology*, 15, 1999-2011, 2014.
- 659
- 660 Perica, S., D. Martin, S. Pavlovic, I. Roy, M. St. Laurent, C. Trypaluk, D. Unruh, M. Yekta,
661 and G. Bonnin NOAA Atlas 14 precipitation- frequency Atlas of the United States Volume 9
662 Version 2.0: Southeastern States (Alabama, Arkansas, Florida, Georgia, Louisiana,
663 Mississippi), 2013. 2013.
- 664
- 665 Pilgrim, D.: Section 1 - Flood routing, in *Australian Rainfall and Runoff - A Guide to Flood*
666 *Estimation*, 1997. 1997.
- 667
- 668 Prudhomme, C. and Davies, H.: Assessing uncertainties in climate change impact analyses on
669 the river flow regimes in the UK. Part 2: future climate, *Climatic Change*, 93, 197-222, 2009.
- 670
- 671 Prudhomme, C., Reynard, N., and Crooks, S.: Downscaling of global climate models for
672 flood frequency analysis: where are we now?, *Hydrological processes*, 16, 1137-1150, 2002.
- 673
- 674 Rivard, G.: Design Storm Events for Urban Drainage
675 Based on Historical Rainfall Data: A Conceptual
676 Framework for a Logical Approach, *Journal of Water Management Modeling*, R191-12, 187-
677 199, 1996.
- 678 Schreider, S. Y., Smith, D. I., and Jakeman, A. J.: Climate Change Impacts on Urban
679 Flooding, *Climatic Change*, 47, 91-115, 2000.



- 680 Seneviratne, S. I., Nicholls, N., Easterling, D., Goodess, C. M., Kanae, S., Kossin, J., Luo, Y.,
681 Marengo, J., McInnes, K., and Rahimi, M.: Changes in climate extremes and their impacts on
682 the natural physical environment, *Managing the risks of extreme events and disasters to*
683 *advance climate change adaptation*, 2012. 109-230, 2012.
- 684
- 685 Singh, V. P. and Woolhiser, D. A.: Mathematical modeling of watershed hydrology, *Journal*
686 *of hydrologic engineering*, 7, 270-292, 2002.
- 687
- 688 Smith, B. K., Smith, J., and Baeck, M. L.: Flash Flood–Producing Storm Properties in a
689 Small Urban Watershed, *Journal of Hydrometeorology*, 17, 2631-2647, 2016.
- 690
- 691 Thodsen, H.: The influence of climate change on stream flow in Danish rivers, *Journal of*
692 *Hydrology*, 333, 226-238, 2007.
- 693
- 694 Trenberth, K. E.: Changes in precipitation with climate change, *Climate Research*, 47, 123-
695 138, 2011.
- 696 United Nations, D. o. E. a. S. A., Population Division: *World Urbanization Prospects: The*
697 *2014 Revision, Highlight*, 2014. 2014.
- 698
- 699 Utsumi, N., Seto, S., Kanae, S., Maeda, E. E., and Oki, T.: Does higher surface temperature
700 intensify extreme precipitation?, *Geophysical Research Letters*, 38, 2011.
- 701
- 702 Victor Mockus, W. H. M., Helen Fox Moody, Donald and E. Woodward, C. C. H., Quan D.
703 Quan: *National Engineering Handbook Chapter 4- Storm Rainfall Depth and Distribution*,
704 2015. 2015.
- 705
- 706 Wasko, C., Parinussa, R., and Sharma, A.: A quasi- global assessment of changes in
707 remotely sensed rainfall extremes with temperature, *Geophysical Research Letters*, 2016a.
708 2016a.
- 709
- 710 Wasko, C. and Sharma, A.: Continuous rainfall generation for a warmer climate using
711 observed temperature sensitivities, *Journal of Hydrology*, 544, 575-590, 2017.
- 712
- 713 Wasko, C. and Sharma, A.: Quantile regression for investigating scaling of extreme
714 precipitation with temperature, *Water Resources Research*, 50, 3608-3614, 2014.
- 715
- 716 Wasko, C. and Sharma, A.: Steeper temporal distribution of rain intensity at higher
717 temperatures within Australian storms, *Nature Geosci*, 8, 527-529, 2015.
- 718
- 719 Wasko, C., Sharma, A., and Johnson, F.: Does storm duration modulate the extreme
720 precipitation- temperature scaling relationship?, *Geophysical Research Letters*, 42, 8783-
721 8790, 2015.
- 722
- 723 Wasko, C., Sharma, A., and Westra, S.: Reduced spatial extent of extreme storms at higher
724 temperatures, *Geophysical Research Letters*, 43, 4026-4032, 2016b.
- 725
- 726 Westra, S., Alexander, L. V., and Zwiers, F. W.: Global Increasing Trends in Annual
727 Maximum Daily Precipitation, *Journal of Climate*, 26, 3904-3918, 2013a.



- 728 Westra, S., Evans, J. P., Mehrotra, R., and Sharma, A.: A conditional disaggregation
729 algorithm for generating fine time-scale rainfall data in a warmer climate, *Journal of*
730 *Hydrology*, 479, 86-99, 2013b.
731
- 732 Wilks, D. S.: Use of stochastic weathergenerators for precipitation downscaling, Wiley
733 *Interdisciplinary Reviews: Climate Change*, 1, 898-907, 2010.
734
- 735 Woldemeskel, F. M., Sharma, A., Mehrotra, R., and Westra, S.: Constraining continuous
736 rainfall simulations for derived design flood estimation, *Journal of Hydrology*, 542, 581-588,
737 2016.
738
- 739 Zhou, Q., Leng, G., and Huang, M.: Impacts of future climate change on urban flood risks:
740 benefits of climate mitigation and adaptations, *Hydrology and Earth System Sciences*
741 *Discussions*, doi: 10.5194/hess-2016-369, 2016. 1-31, 2016.
742
- 743 Zhou, X., Bai, Z., and Yang, Y.: Linking trends in urban extreme rainfall to urban flooding in
744 China, *International Journal of Climatology*, doi: 10.1002/joc.5107, 2017. 2017.
745
- 746 Zope, P. E., Eldho, T. I., and Jothiprakash, V.: Impacts of land use–land cover change and
747 urbanization on flooding: A case study of Oshiwara River Basin in Mumbai, India,
748 *CATENA*, 145, 142-154, 2016.
749
- 750 Zoppou, C.: Review of urban storm water models, *Environmental Modelling & Software*, 16,
751 195-231, 2001.
- 752
- 753
- 754